

MIT Open Access Articles

Cell-free expression, purification, and ligand-binding analysis of Drosophila melanogaster olfactory receptors DmOR67a, DmOR85b and DmORCO

The MIT Faculty has made this article openly available. **Please share** how this access benefits you. Your story matters.

Citation: Tegler, Lotta Tollstoy, Karolina Corin, Julia Hillger, Brooke Wassie, Yanmei Yu, and Shuguang Zhang. "Cell-Free Expression, Purification, and Ligand-Binding Analysis of Drosophila Melanogaster Olfactory Receptors DmOR67a, DmOR85b and DmORCO." Sci. Rep. 5 (January 19, 2015): 7867.

As Published: <http://dx.doi.org/10.1038/srep07867>

Publisher: Nature Publishing Group

Persistent URL: <http://hdl.handle.net/1721.1/94533>

Version: Final published version: final published article, as it appeared in a journal, conference proceedings, or other formally published context

Terms of use: Creative Commons Attribution





OPEN

SUBJECT AREAS:
EXPRESSION SYSTEMS
MEMBRANE PROTEINSReceived
8 July 2014Accepted
11 December 2014Published
19 January 2015Correspondence and
requests for materials
should be addressed to
L.T.T. (lotta.tollstoy.
teglor@liu.se)* These authors
contributed equally to
this work.Cell-free expression, purification, and
ligand-binding analysis of *Drosophila
melanogaster* olfactory receptors
DmOR67a, DmOR85b and DmORCOLotta Tollstoy Teglör^{1,2*}, Karolina Corin^{1,3,4*}, Julia Hillger¹, Brooke Wassie¹, Yanmei Yu^{1,5}
& Shuguang Zhang¹

¹Center for Bits and Atoms, Massachusetts Institute of Technology, 77 Massachusetts, Cambridge, MA 02139-4307, USA, ²Division of Chemistry, Department of Physics, Chemistry and Biology, Linköping University, SE-581 83 Linköping, Sweden, ³Biomedical Engineering Research Group, School of Electrical and Information Engineering University of the Witwatersrand, Johannesburg, South Africa, ⁴Department of Molecular Medicine and Haematology, University of the Witwatersrand, Johannesburg, South Africa, ⁵College of Electronics and Information Engineering, Sichuan University, Chengdu, China 610065.

Insects transmit numerous devastating diseases, including malaria, dengue fever, and sleeping sickness. Olfactory cues guide insects to their hosts, and are thus responsible for disease transmission. Understanding the molecular basis of insect olfaction could facilitate the development of interventions. The first step is to heterologously overexpress and purify insect olfactory receptors (ORs). This is challenging, as ORs are membrane proteins. Here, we show that insect ORs and their co-receptor can be expressed in an *E. coli* cell-free system. After immunoaffinity chromatography, the ORs are ~95% pure, and up to 1 mg/10 ml reaction is obtained. Circular dichroism together with microscale thermophoresis indicate that each receptor is properly folded, and can bind its respective ligand. This is the first time insect ORs have been expressed in an *E. coli* system. The methods described here could facilitate future structure-function studies, which may aid in developments to alleviate the suffering of millions caused by insect-transmitted diseases.

The insect olfactory system is unique among animal olfactory systems. Unlike mammalian, fish, and nematode olfactory receptors (ORs), insect ORs are not GPCRs. Relative to other ORs, insect ORs have an inverted topology, with an intracellular N-terminus and extracellular C-terminus^{1,2}. This inverted orientation allows them to form a heteromeric complex via intracellular domains¹, which functions as an odorant-gated ion channel^{3,4}. Each heteromeric complex is comprised of a unique odorant-detecting OR, and the ubiquitously expressed Orco. The Orco sequence is highly conserved among insect species⁵, and is necessary to target the complex to olfactory neuron dendrites^{1,6}. Moreover, its presence is required for ion channel function^{3,4}.

While significant progress has been made in understanding the insect olfactory system, relatively little is known about how the ORs function at the molecular level. One study was able to show that residues between transmembrane 3 and the second extracellular loop are involved in odorant recognition⁷, while another demonstrated that a V91A mutation in the predicted second transmembrane region could confer resistance to DEET in DmOR59b⁸. A third study showed that the second extracellular loop likely forms β -turns which may be critical for olfactory function in all insects⁹, while a fourth study demonstrated that a single residue mutation in the third transmembrane domain was sufficient to alter species-specific pheromone sensitivity¹⁰. To the best of our knowledge, no such other structure-function studies have been published. However, if the molecular basis of insect olfaction was elucidated, hundreds of millions of people worldwide could be spared from debilitating illnesses. Insects like mosquitoes, tsetse flies, and sandflies are vectors for numerous diseases, including malaria, yellow fever, dengue fever, and sleeping sickness¹¹. Volatile odors emitted by humans allow these insects to trace and infect their hosts. If the insect OR structure-function relationship was understood, it might be possible to design compounds that could disrupt insects' ability to trace humans, that could redirect or efficiently trap insects, or that could possibly even prevent disease-carrying insects from mating.

Insect OR expression and purification is a prerequisite for structure-function studies, especially if a molecular structure is desired. However, such studies have been limited. The receptors DmOR22a and DmORCO (also



known as DmOR83b) were successfully expressed in and purified from SF9 insect cells and a wheat-germ cell-free system, while DmOR22a, DmOR35a, and DmOR43b could be expressed in the same systems¹². These authors found that neither *E. coli* cells, nor an *E. coli* cell-free system, could be used to express full-length receptors. Another study was able to use a rabbit reticulocyte cell-free system to express DmORCO². However, neither study performed ligand-binding experiments to show that the expressed receptors were biologically functional. Here, we show that full-length drosophila ORs can indeed be expressed in an *E. coli* cell-free system. The success of insect OR expression in *E. coli* systems likely depends on the reaction conditions, including the presence of an optimal detergent. Circular dichroism and microscale thermophoresis indicate that the expressed receptors are properly folded and can bind their small odorant ligands. Moreover, the receptors are pure enough for downstream structure and function analyses, including crystal screens.

Results

Cell-Free Drosophila Olfactory Receptor Expression and Purification. *E. coli*-based cell-free expression systems were successfully used to express the insect olfactory receptors DmOR67a, DmOR85b, and DmORCO. As previously shown with mammalian ORs, the optimal detergent was Brij-35 at a concentration of 0.2% w/v¹³. At this concentration, approximately 70–93% of the expressed receptors were soluble (Figure 1). However, unlike mammalian ORs, the reaction temperature could affect the solubility and yield of the insect ORs. The optimal temperature, which maximized both receptor yield and solubility, was found to be 33°C for DmOR67a and DmOR85b (Figure 1). The solubility of DmORCO was not affected by changes of temperature within this range, while expression was highest at 33°C or 37°C. The yield of insect ORs was comparable, though generally less than that of mammalian ORs. Mouse, human, or rat ORs could be expressed at levels of ~0.5–7 mg in each 10 ml *E. coli* cell-free batch reaction^{13–15}. In contrast, the average yields of DmOR67a were ~0.5 mg/10 ml, the average yields of DmORCO were ~0.8 mg/10 ml, and the average yields for DmOR85b were ~0.9 mg/10 ml.

Western blots confirmed full-length expression of the receptors (Figure 2). DmOR67a ran at about 38 kDa, DmOR85b ran at about 35 kDa, and DmORCO ran at about 47 kDa. Although these sizes are less than the predicted sizes of 47 kDa (DmOR67a), 45.6 kDa (DmOR85b), and 54.4 kDa (DmORCO), previous studies have shown that membrane proteins tend to migrate faster on gels than their true molecular weights^{13–18}. It has been hypothesized that this may be due to incomplete denaturation by SDS¹⁶. However, western blot detection against the C-terminal 1D4 tag suggests full-length receptor expression. Moreover, a previous study found that full-length purified DmORCO ran just under 50 kDa¹², which is consistent with the results reported here.

A monoclonal antibody against the C-terminal 1D4 tag was used to purify the expressed receptors, and silver stains were used to assay their purity. The silver stains showed that the expressed receptors were >95% pure, and ran at the same sizes observed in the Western blots (Figure 3). The high degree of purity was obtained after washing the bead-bound receptors with 22 times the bead volume prior to eluting them, and made them suitable for numerous downstream analyses, including crystal screens. The Western blots of DmOR67a and DmORCO in Figure 2, and all of the silver stains in Figure 3, showed only single bands, while a Western blot of DmOR85b showed three bands, one dominant band at 35 kDa and two faint bands at higher molecular weights (Figure 2). The second band was at approximately ~50 kDa. This slower migration could be due to partial denaturation by SDS. The third band was approximately twice the molecular weight of the first band. Although this might suggest that DmOR85b is capable of homodimerization in

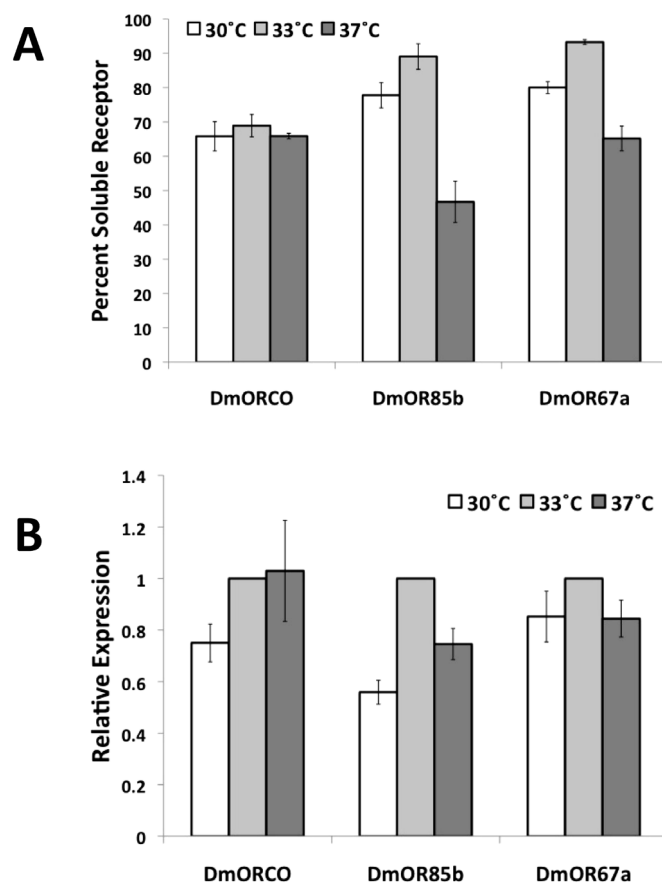


Figure 1 | Expression of insect olfactory receptors from *E. coli*-based cell-free expression reactions. (A) Percentage of soluble receptor at 30°, 33°, and 37°C. DmOR85b and DmOR67a are most soluble at 33°C. The temperature does not affect DmORCO solubility. (B) Relative expression of DmORCO, DmOR85b, and DmOR67a at 30°, 33°, and 37°C. The expression of each sample was normalized to the expression at 33°C. The expression of DmORCO is highest at 33°C or 37°C. Higher yields of DmOR85b and DmOR67a are obtained at 33°C. The temperature 33°C maximizes both expression and solubility of 2 receptors, and is not a critical factor for the third. Thus, this temperature was chosen for all experiments. Error bars show \pm S.E.M. Number of replicates (N) = 2 for DmOR85b at 30 C in B, N = 3–5 for all other data points.

this system, it is more likely that this band is also an artifact of incomplete denaturation, or the result of receptor aggregation on the gel, and further studies are necessary. This is in contrast with mammalian ORs, and even other GPCRs, where homodimerization has consistently been observed^{13–21}. Due to potential aggregation of DmOR85b, this receptor was run through a size-exclusion column on an ÄKTA purifier before ligand binding experiments. Aggregates or dimer were not detectable in the chromatogram. The peak for the monomeric protein was collected and concentrated prior to further experiments.

Secondary Structure Analysis Using Circular Dichroism. Circular dichroism was used to analyze the secondary structure of the purified receptors. Although insect ORs have a different topology than mammalian ORs, with an intracellular N-terminus and an extracellular C-terminus, they are still predicted to have seven transmembrane alpha helices^{1,2,7,22}. The spectra for all three receptors are typical for alpha helical proteins (Figure 4). The spectra for DmOR67 and DmOR85b nearly overlap, while the spectrum for DmORCO indicates a higher helical content²³. A similar difference in spectra between DmORCO and other DmORs as been reported for receptors synthesized in SF9

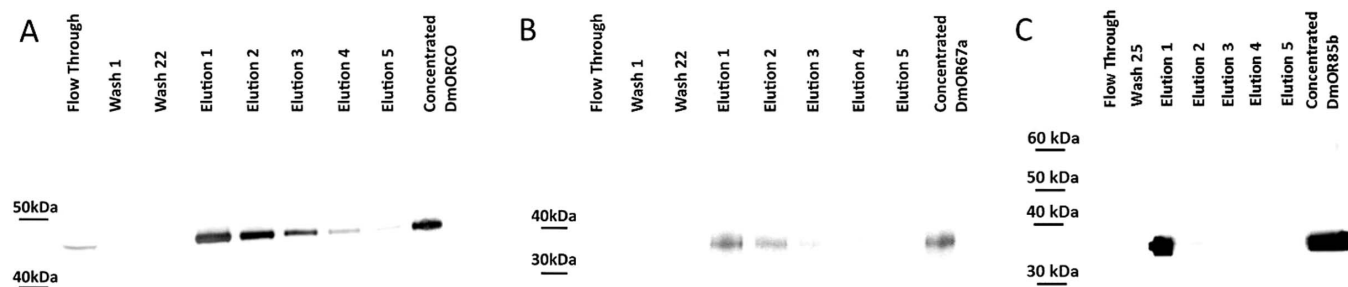


Figure 2 | Western blots of DmOR67a, DmORCO, and DmOR85b. (A) Western blot of DmOR67a. A single band is detected at ~ 38 kDa against the C-terminal rho 1D4 tag, indicating full-length expression. Most of the expressed receptor is recovered in the first elution, and all detectable receptor is recovered by the fifth elution. (B) Western blot of DmORCO. A single band is detected at ~ 47 kDa, indicating full-length expression. Like DmOR67a, most of the receptor is recovered in the first elution, and five are required to fully elute the protein. (C) Western blot of DmOR85b. Three bands are seen, a dominant band at ~ 35 kDa and two faint bands at ~ 50 kDa, and ~ 60 kDa. The ~ 35 kDa and ~ 60 kDa bands may suggest monomeric and potential dimeric forms. However, the ~ 60 kDa band more likely results from receptor aggregation, or incomplete SDS denaturation. The ~ 50 kDa band is most likely the result of a slower migration speed due to incomplete SDS denaturation.

cells or in a wheat germ cell-free system¹². This consistency of results across independent studies under different experimental conditions suggests that the *E. coli*-expressed receptors are comparable to those expressed in other systems. Furthermore, this data, in conjunction with the ligand-binding experiments, suggests that the receptors are properly folded.

Ligand Binding Analysis Using Microscale Thermophoresis. The ability of the purified DmORs to bind their respective ligands was analyzed using microscale thermophoresis. DmOR67a and DmORCO were titrated individually and together with ethyl benzoate, while DmOR85b and DmORCO were titrated individually and together with 2-heptanone. As an additional control, a reciprocal binding experiment was performed, with DmOR67a and DmORCO titrated against 2-heptanone, and DmOR85b and DmORCO titrated against ethyl benzoate.

When DmOR67a was co-incubated with DmORCO, binding to ethyl benzoate was detected with an affinity of $\sim 0.5 \pm 0.1 \mu\text{M}$

(Figure 5A). Similarly, when DmOR85b was co-incubated with DmORCO, binding to 2-heptanone was seen with an affinity of $\sim 0.8 \pm 0.2 \mu\text{M}$ (Figure 5B).

When each receptor was individually exposed to either ligand, no or lower affinity binding was seen. Similar results were observed in a negative control reciprocal binding experiment, where co-incubated receptors were titrated with non-native ligands. Binding curves with K_D 's of $\sim 1.2 \mu\text{M}$ and $\sim 0.7 \mu\text{M}$ could be fit to both DmOR67a with ethyl benzoate, and DmOR85b with 2-heptanone, respectively (Figures 5C and 5D). This is not surprising, given that DmOR67a and DmOR85b are the ligand-binding domains: some binding could conceivably be expected even when this domain is not in the presence of DmORCO. However, the variance of error was significantly higher in these experiments, and goodness-of-fit tests demonstrated that the model fits were poor relative to those where each receptor was co-incubated with DmORCO (Supplementary Table 1). The high noise, yet similar binding affinities to those measured in Figures 5A and 5B, could suggest that some weaker binding is occurring, but that the

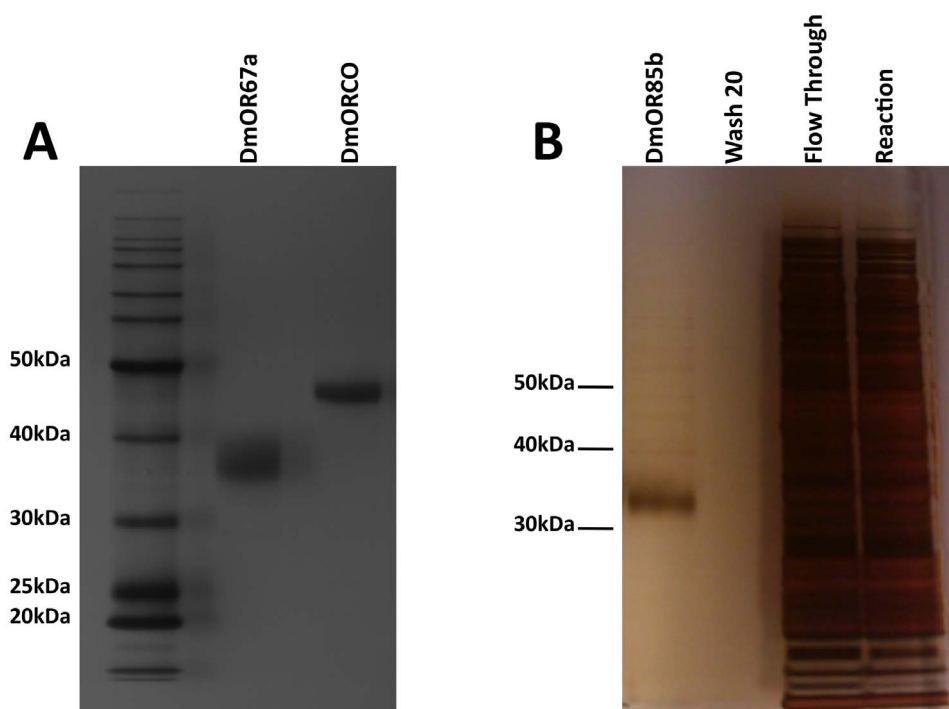


Figure 3 | Silver stains of purified DmOR67a, DmORCO, and DmOR85b. (A) Silver stains of purified DmOR67a and DmORCO. The purified receptors are $>95\%$ pure. (B) Silver stain of DmOR85b before and after purification. Only a monomeric band at ~ 35 kDa is detected after purification. Full silver stains are shown in Supplementary Figures 1 and 2.

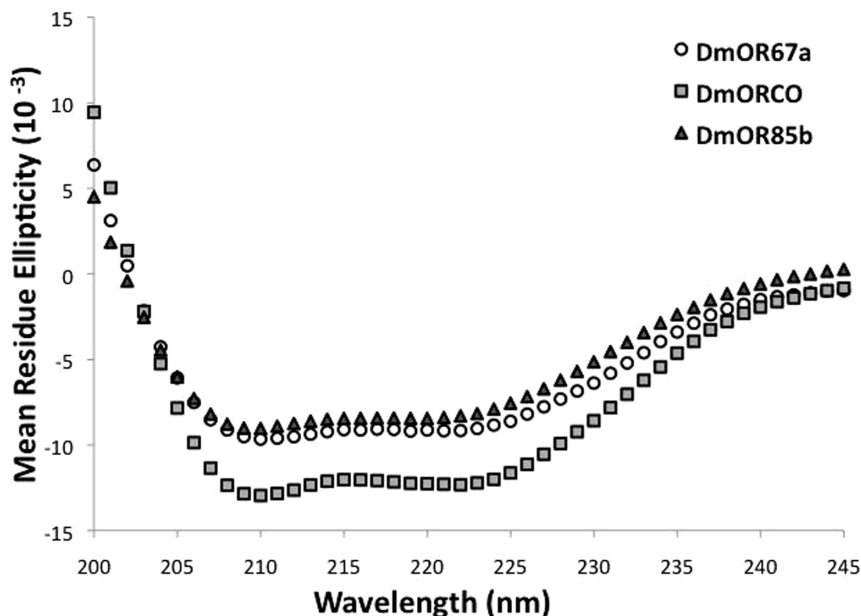


Figure 4 | Circular dichroism spectra of DmOR67a, DmORCO, and DmOR85b. Each receptor has a helical spectrum, indicating that they are properly folded. DmOR67a and DmOR85b have similar helical content, while DmORCO has a higher helical content.

DmORCO subunit is required to make the odorant-binding subunits fully functional. Similarly, either no binding, or no statistically significant binding, was detected when DmORCO was titrated with 2-heptanone (Figure 5F), when DmOR67a was co-incubated with DmORCO and titrated with 2-heptanone (Figure 5G), or when DmOR85b was co-incubated with DmORCO and titrated with ethyl benzoate (Figure 5H) (Supplementary Table 1). Curiously, some binding was detected when DmORCO was titrated with ethyl benzoate (Figure 5G). The measured affinity was over one order of magnitude higher than that measured in Figures 5A and 5B, and the difference between high and low plateaus nearly half, suggesting that any binding may be non-specific. However, it should be noted that, while DmORCO has thus far not been shown to bind to odorants, direct binding to agonists has recently been demonstrated^{24,25}. These agonists contain a ring structure like ethyl benzoate. Thus, the possibility of DmORCO binding directly to ethyl benzoate should not be excluded.

Taken together, this data suggests that the expressed and purified receptors are capable of ligand-binding. Previous reports demonstrated that insect olfactory neurons express a unique olfactory receptor together with the ubiquitous DmORCO^{5,26}. These proteins form a complex, which acts as an odorant-gated ion channel, and where the unique OR forms the odorant-binding subunit^{1,3,4,27}. Because definitive binding with sufficiently high affinity is only seen when the two receptor subunits are co-incubated and titrated with their native ligands, this data indicates that drosophila olfactory receptors can be purified in an active form. It further supports the notion that a complex formed from both a unique DmOR and DmORCO is necessary to detect scent.

Discussion

Expression, solubilization, and purification are prerequisites for membrane protein structure-function studies. This study documents the first ever expression and purification of the insect olfactory receptors DmOR67a and DmOR85b, and the first time DmORCO has been expressed and purified from an *E. coli* cell-free system. Moreover, it is the first time that ligand-binding studies have been conducted on any purified insect ORs. Interestingly, previous reports found that full-length insect OR expression couldn't be obtained in *E. coli*-based systems¹². As different ORs were used in this study, it's

possible that only specific insect ORs can be expressed in *E. coli* systems. However, the experimental conditions are more likely to affect expression. Truncated expression products were found when insect ORs had an N-terminal maltose binding protein (MBP) tag¹². The ORs in this study did not have an N-terminal tag, but were expressed at full-length as evidenced by their molecular weight and antibody detection against the C-terminal rho-tag. This suggests that the MBP tag, or perhaps even any N-terminal tag, may interfere with expression of insect ORs.

Membrane proteins must be solubilized in detergents in order to maintain their structure and function. We were able to solubilize up to ~90% of the expressed insect ORs by adding Brij-35 directly to the reactions at a concentration of 0.2% w/v. While Brij-35 or other detergents have been used to solubilize insect ORs expressed in cell-free systems¹², they were only used *after* synthesis in a wheat-germ system at concentrations of 1–5%. As a result, only the harshest detergents could solubilize most of the synthesized receptors. No detergent was added directly to an *E. coli* cell-free system prior to receptor synthesis. Adding the detergent directly allows for solubilization immediately upon expression, and may facilitate the use of milder detergents. It also decreases the number of necessary experimental steps, and minimizes the potential need for re-folding protocols.

The yields of all three receptors are comparable to published yields for other insect and mammalian ORs^{12–15}, ranging from ~0.5–1 mg of purified receptor per 10 ml of cell free reaction. While this is sufficient for most structure and function studies, even higher yields would be optimal for crystal screens. It might be possible to increase the amount of expressed receptor with a continuous flow protocol instead of batch expression. Alternatively, further research into solubilization and stabilization protocols, e.g. with nanodisc particles or peptide detergents^{14,15,28–30}, could potentially increase the quantity of receptor that is functionally available after purification.

Circular dichroism and microscale thermophoresis in tandem indicate that all three receptors in this study were properly folded, and were able to bind their reported ligands. The circular dichroism spectra of the receptors in this study matched those of *Drosophila* ORs made in SF9 cells or a wheat germ cell-free system¹². Although this is the first time binding affinities have been measured for purified insect ORs, the values are in good agreement with purified mam-

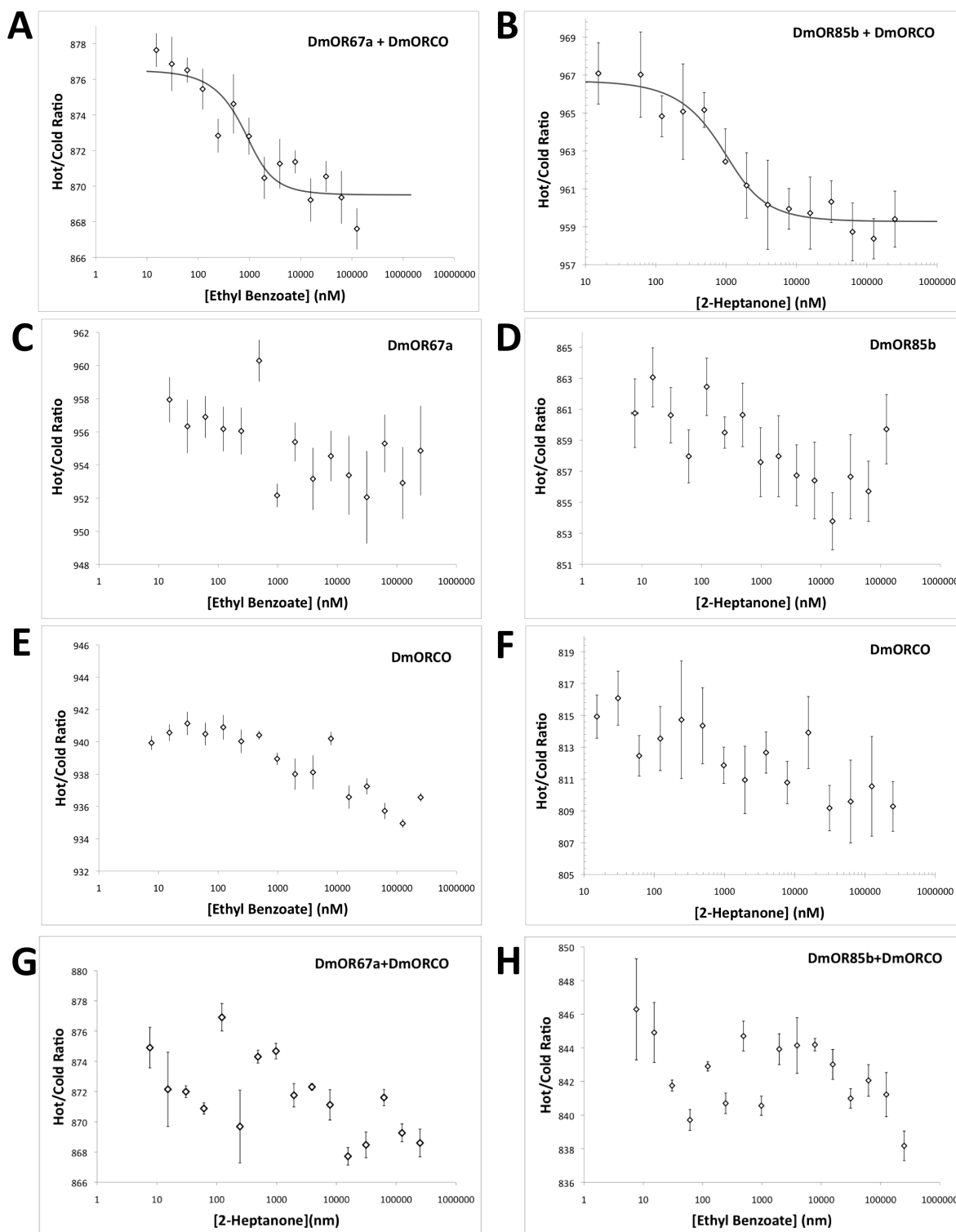


Figure 5 | Microscale thermophoresis ligand-binding data for DmOR67a and DmORCO with ethyl benzoate, and DmOR85b and DmORCO with 2-heptanone. The binding data are presented as hot/cold ratios. This ratio measures the difference in fluorescence signal before (cold) and after (hot) a local thermal gradient is applied. The change in ratio is caused by a change in thermophoretic motion due to a binding event³². (A) Distinct ligand binding is seen when DmOR67a and DmORCO are co-incubated with ethyl benzoate, a known ligand for DmOR67a. The measured affinity is $\sim 0.5 \pm 0.1 \mu\text{M}$. (B) Binding is also seen when DmOR85b and DmORCO are co-incubated with 2-heptanone, a known ligand for DmOR85b. The measured affinity is $\sim 0.8 \pm 0.2 \mu\text{M}$. (C) Microscale thermophoresis data for DmOR67a titrated alone with ethyl benzoate. (D) Microscale thermophoresis data for DmOR85b titrated alone with 2-heptanone. (E) Microscale thermophoresis data for DmORCO titrated alone with ethyl benzoate. (F) Microscale thermophoresis data for DmORCO titrated alone with 2-heptanone. (G) Microscale thermophoresis data for DmOR67a co-incubated with DmORCO and titrated against the non-native ligand 2-heptanone. (H) Microscale thermophoresis data for DmOR85b co-incubated with DmORCO and titrated against the non-native ligand ethyl benzoate. Binding curves are not shown in (C) – (G) because of poor fits (C, D, F, G) or because any binding was not significant relative to that seen in A or B (student's T-test, $p \leq 0.01$) (E). No curve could be fit for (H). Curve-fitting analyses are shown in the supplementary information.



malian ORs, which typically have micromolar binding affinities^{13,14,17,31,32}. Indeed, micromolar binding would be expected for olfactory receptors, as animals typically use them to continuously detect environmental cues in real-time. However, it should be noted that the affinity measured for purified DmOR85b is higher than that measured when the same receptor is expressed in xenopus oocytes: when DmOR85b is co-expressed in oocytes with DmORCO, it responds to 2-heptanone with an EC₅₀ of 70 μM⁷. This difference in values is likely to be due to differences in the measurement systems used. In oocytes, the value more accurately reflects the odorant concentration necessary to induce a signal response in cells. With purified receptors, the value is more likely to reflect actual binding of the odorant to the receptor.

Taken together, this study demonstrates that *E. coli* cell-free systems can be used to express insect ORs, which can subsequently be purified to a high degree. This system may prove advantageous over other systems, with easier protocols, shorter production times, and higher relative yields (0.5–1 mg/10 ml compared to 5–6 mg/L in SF9 cells)¹². Indeed, *E. coli* cell-free expression is a tool that can greatly facilitate insect OR structure and function studies.

Methods

Drosophila Olfactory Receptor Vector Design. A cDNA clone of DmOR85b was a kind gift from Charles W. Luejche's lab. The sequences for the DmORCO (accession Q9VNB5) and DmOR67a (accession Q9VT08) genes were obtained from Pubmed, optimized for *E. coli* expression, and synthesized by Gen9 Inc, Cambridge, MA, USA. For each OR, a C-terminal 1D4 tag was added for detection and purification, as well as a 3' NcoI site and a 5' XhoI site for cloning. The restriction sites and 1D4 tag were either synthesized directly (DmOR67a and DmORCO), or added using PCR (DmOR85b) (Forward: TATATAGAATTCGAGGAGGGCCACCATGGAGAA-GCTAATGAAGTACGC; Reverse: TATATACTCGAGTTATTAAGCTGGCGC-CACCTGGGAAGTCTCGGTGCCGGAGGAGCCTTGGGTATACATTGT-GCGC). All OR DNA sequences were cloned into the pIVex2.3d vector using the restriction sites and transformed into chemically competent DH5α cells (Invitrogen, Life Technologies, Grand Island, NY, USA). The plasmids were amplified and extracted (Qiagen Plasmid Mini or Maxi kits; Qiagen, Germantown, MD, USA), and the sequences were verified using plasmid specific primers (Forward: CGACTCACTATAGGGAGACC; Reverse: TAGTAACGGCCGCCAGTGTGCTG).

Cell-free dmOR Expression. *E. coli* based cell-free expression kits were used to synthesize the ORs according to the manufacturer's instructions (32506, Qiagen; RiNA GmbH, Berlin, Germany), with the exception that reactions were performed at 33°C unless stated otherwise. To compensate for the lack of a natural membrane, the surfactant Brij-35 (Anatrace, Maumee, OH, USA) was added directly to the reactions at a concentration of 0.2% w/v. After the reactions were complete, the samples were centrifuged at 10,000 rpm for 10 minutes. The supernatant containing the solubilized protein was removed for further analysis. Final reaction volumes of 0.5–5 ml were used to produce protein that was purified for secondary structure and binding analyses.

Dot Blot and Western Blot Detection, and Total Protein Staining. Dot blots, western blots, and silver stains were used to detect the proteins and analyze their purity. For dot blots, the samples were pipetted directly onto a nitrocellulose membrane and allowed to air dry for 10–20 minutes. For western blots and silver stains, samples were prepared and loaded in Novex 10% Bis-Tris SDS-PAGE gels (Invitrogen, Life Technologies) according to the manufacturer's instructions, with the exception that the samples were incubated at room temperature prior to loading as boiling causes membrane protein aggregation. For blotting, the gel-resolved samples were transferred to a nitrocellulose membrane (iBlot, Life Technologies). The dot blots and western blots were blocked in milk (5% w/v non-fat dried milk in TBST, 1 hour at room temperature or overnight at 4°C), and incubated with a rho1D4 primary antibody (Cell Essentials, Boston, MA, USA) (0.5 μg/ml in TBST, 1 hour at room temperature or overnight at 4°C). The ORs were then detected with a goat anti-mouse HRP-conjugated secondary antibody (32430, Thermo Fisher Scientific Inc., Rockford, IL, USA) (1 : 5000 in TBST, 1 hour, room temperature) and visualized using the ECL-Plus Kit (GE Healthcare Bio-Sciences, Pittsburgh, PA, USA). The SilverXpress kit (Life Technologies, LC6100) was used according to the manufacturer's instructions to perform total protein stains of the samples. All images were captured using a Fluor Chem gel documentation system (Alpha Innotech, San Leandro, CA, USA). ImageJ software³³ was used to compare dot or band intensities and analyze sample purity.

Rho1D4 Monoclonal Antibody Immunoaffinity Purification. CNBr-activated Sepharose 4B beads (GE Healthcare, 17-0430) chemically linked to the rho1D4 monoclonal antibody (Cell Essentials) were used for immunoaffinity purification. Solubilized protein from the cell-free reactions was mixed with the bead slurry (binding capacity 0.7 mg/ml) and reacted overnight at 4°C to capture the synthesized

protein. DNase I (1 : 1000, Life Technologies, 18047019) and RNase A (1 : 1000, Life Technologies, 12091021) were added to the overnight rotations. The beads were then washed with wash buffer (PBS + 0.2% FC-14 w/v) until spectrophotometer readings indicated that all excess protein had been removed (<0.01 mg/ml). The captured ORs were eluted with elution buffer (PBS + 0.2% FC-14 + 800 μM elution peptide). Elutions were performed until spectrophotometer readings indicated that no more protein was present (<0.01 mg/ml). The protein was concentrated using 30 kDa or 50 kDa MWCO filter columns (Millipore, Billerica MA, USA). All concentrations were measured using the NanoDrop 1000 spectrophotometer (Thermo Scientific, Wilmington, DE, USA). The beads were pelleted by centrifugation at 1,400 g for one minute between each wash and elution. The detergent was switched to fos-choline 14 for receptor purification and all subsequent experiments because it has previously been shown to be optimal for receptor purification^{13–16}. The Fos-choline-14 (n-Tetradecylphosphocholine, FC-14) was from Affymetrix (Santa Clara, CA, USA), and the elution peptide Ac-TETSQVAPA-CONH₂ was synthesized by CPC Scientific Inc., Sunnyvale, CA, USA.

Size exclusion chromatography of DmOR85b. Size exclusion chromatography was used to separate the monomeric and potential higher molecular-weight forms of the receptor DmOR85b. A Hi-Load 16/60 Supradex 200 column, equilibrated with wash buffer and connected to an Akta Purifier HPLC system (GE Healthcare) was used. The protein was sample loaded on the column, and run with wash buffer at 0.3 ml/min. Fractions exiting the column were automatically collected; protein content was monitored with UV absorbance at 215 nm, 254 nm, and 280 nm. Peak fractions were pooled, concentrated, and analyzed by silver staining (SilverXpress, Invitrogen). A calibration to correlate the retention time with the molecular mass was previously performed in our lab, and is described in Ref. 32.

Secondary Structure Analysis with Circular Dichroism. Circular dichroism spectra were recorded on a CD spectrometer (model 410, Aviv Biomedical, Lakewood Township, NJ, USA) at 15°C over the wavelength range of 195–250 nm with a step size of 1 nm and an averaging time of 4 seconds. Spectra for purified ORs were recorded in and blanked to wash buffer (DPBS with 0.2% FC-14 w/v). A 111-QS quartz sample cell with a path length of 1 mm (Hellma USA, Plainview, NY, USA) was used. For each experiment, 300 μl of protein sample was used with a concentration of 0.1 mg/ml. The spectra were smoothed using an averaging filter with a span of 5.

Microscale Thermophoresis Ligand-Binding Analysis. Microscale thermophoresis was used to measure the binding interactions between purified receptors and their ligands using a setup similar to that previously described^{13,34}. The receptor DmOR67a was titrated with Ethyl Benzoate and DmOR85b was titrated with 2-Heptanone. Both receptors were tested in the presence and absence of DmORCO. As controls, samples of only DmORCO were titrated with both odorants, and a reciprocal binding experiment with non-native ligands was also performed. Each receptor was at a concentration of 1 μM. The final concentrations of ethyl benzoate and 2-heptanone were: 250, 125, 62.5, 31.3, 15.6, 7.81, 3.91, 1.95, 0.98, 0.49, 0.24, 0.12, 0.061, 0.031, and 0.015 μM in 0.5% DMSO. All samples were loaded into standard coated label-free capillaries in a buffer solution of 0.2% FC-14 in PBS. All tests were repeated 3–8 times, and run on a MonolithNT label-free instrument (NanoTemper GmbH, Munich, Germany) with 17% LED power and 40% MST power. Data points were fit to the inverse Hill equation. To determine whether the fitted curves indicated that significant binding was occurring, the AIC (Akaike Information Criterion) and pseudo-R² were computed for each best-fit curve. A T-test was used to compare the significance of binding between different experiments.

- Benton, R., Sachse, S., Michnick, S. W. & Vosshall, L. B. Atypical membrane topology and heteromeric function of *Drosophila* odorant receptors in vivo. *PLoS Biol.* **4**, e20 (2006).
- Lundin, C. *et al.* Membrane topology of the *Drosophila* OR83b odorant receptor. *FEBS Lett.* **581**, 5601–04 (2007).
- Wicher, D. *et al.* *Drosophila* odorant receptors are both ligand-gated and cyclic-nucleotide-activated cation channels. *Nature* **452**, 1007–11. (2008).
- Sato, K. *et al.* Insect olfactory receptors are heteromeric ligand-gated ion channels. *Nature* **452**, 1002–06 (2008).
- Krieger, J., Klink, O., Mohl, C., Raming, K. & Breer, H. A candidate olfactory receptor subtype highly conserved across different insect orders. *J. Comp. Physiol. A* **189**, 519–26 (2003).
- Larsson, M. C. *et al.* Or83b encodes a broadly expressed odorant receptor essential for *Drosophila* olfaction. *Neuron* **43**, 703–14 (2004).
- Nichols, A. S. & Luetje, C. W. Transmembrane segment 3 of *Drosophila melanogaster* odorant receptor subunit 85b contributes to ligand-receptor interactions. *J. Biol. Chem.* **285**, 11854–62 (2010).
- Pellegrino, M., Steinbach, N., Stensmyr, M. C., Hansson, B. S. & Vosshall, L. B. A natural polymorphism alters odour and DEET sensitivity in an insect odorant receptor. *Nature* **478**, 511–14 (2011).
- Xu, P. & Leal, W. S. Probing insect odorant receptors with their cognate ligands: Insights into structural features. *Biochem. Biophys. Res. Commun.* **435**, 477–82 (2013).



10. Leary, G. P. *et al.* Single mutation to a sex pheromone receptor provides adaptive specificity between closely related moth species. *Proc. Natl. Acad. Sci. USA* **109**, 14081–86 (2012).
11. Carey, A. F. & Carlson, J. R. Insect olfaction: from model systems to disease control. *Proc. Natl. Acad. Sci. USA* **108**, 12987–95 (2011).
12. Carraher, C., Nazmi, A. R., Newcomb, R. D. & Kralicek, A. Recombinant expression, detergent solubilization and purification of insect odorant receptor subunits. *Prot. Expr. Purif.* **90**, 160–69 (2013).
13. Corin, K. *et al.* A robust and rapid method of producing soluble, stable, and functional G-protein coupled receptors. *PLoS ONE* **6**, e23036 (2011).
14. Corin, K. *et al.* Designer lipid-like peptides: A class of detergents for studying functional olfactory receptors using commercial cell-free systems. *PLoS ONE* **6**, e25067 (2011).
15. Wang, X. *et al.* Peptide surfactants for cell-free production of functional G protein-coupled receptors. *Proc. Natl. Acad. Sci.* **108**, 9049–54 (2011).
16. Cook, B. L., Ernberg, K., Chung, H. & Zhang, S. Study of a synthetic human olfactory receptor 17-4: Expression and purification from an inducible mammalian cell line. *PLoS ONE* **3**, e2920 (2008).
17. Corin, K. *et al.* Structure and function analyses of the purified GPCR human vomeronasal type 1 receptor 1. *Sci. Rep.* **1**, 172 (2011).
18. Wang, X., Corin, K., Rich, C. & Zhang, S. Study of two G-protein coupled receptor variants of human trace amine-associated receptor 5. *Sci. Rep.* **1**, 102 (2011).
19. Wu, B. *et al.* Structures of the CXCR4 chemokine GPCR with small-molecule and cyclic peptide antagonists. *Science* **330**, 1066–71 (2010).
20. Leck, K. J., Zhang, S. & Hauser, C. A. E. Study of bioengineered zebra fish olfactory receptor 131-2: Receptor purification and secondary structure analysis. *Plos ONE* **5**, e15027 (2010).
21. Nekrasova, E., Sosinskaya, A., Natchin, M., Lancet, D. & Gat, U. Overexpression, solubilization, and purification of rat and human olfactory receptors. *Eur. J. Biochem.* **238**, 28–37 (1996).
22. Harini, K. & Sowdhamini, R. Molecular modeling of oligomeric states of DmOR83b, an olfactory receptor in *D. melanogaster*. *Bioinform. Biol. Insights* **6**, 33–47 (2012).
23. Greenfield, N. & Fasman, G. D. Computed circular dichroism spectra for the evaluation of protein conformation. *Biochemistry* **8**, 4108–16 (1969).
24. Chen, S. & Leutje, C. W. Identification of new agonists and antagonists of the insect odorant receptor co-receptor subunit. *PLoS One* **7**, e36784 (2012).
25. Jones, P. L., Pask, G. M., Rinker, D. C. & Zwiebel, L. J. Functional agonism of insect odorant receptor ion channels. *Proc Natl Acad Sci* **108**, 8821–8825 (2011).
26. Vosshall, L. B., Amrein, H., Morozov, P. S., Rzhetsky, A. & Axel, R. A spatial map of olfactory receptor expression in the *Drosophila* antenna. *Cell* **96**, 725–736 (1999).
27. Elmore, T., Ignell, R., Carlson, J. R. & Smith, D. P. Targeted mutation of a *Drosophila* odor receptor defines receptor requirement in a novel class of sensillum. *J. Neurosci.* **23**, 9906–12 (2003).
28. McGregor, C. L. *et al.* Lipopeptide detergents designed for the structural study of membrane proteins. *Nat. Biotechnol.* **21**, 171–176 (2003).
29. Yeh, J. I., Du, S., Tordajada, A., Paulo, J. & Zhang, S. Peptergent: peptide detergents that improve stability and functionality of a membrane protein glycerol-3-phosphate dehydrogenase. *Biochemistry* **44**, 16912–16919 (2005).
30. Zhao, X. *et al.* Designer short peptide surfactants stabilize G-protein coupled receptor bovine rhodopsin. *Proc. Natl. Acad. Sci. USA* **103**, 17707–12 (2006).
31. Kaiser, L. K. *et al.* Efficient cell-free production of olfactory receptors: Detergent optimization, structure, and ligand binding analyses. *Proc. Natl. Acad. Sci. USA* **105**, 15726–31 (2008).
32. Cook, B. *et al.* Large-scale production and study of a synthetic G protein-coupled receptor: Human olfactory receptor 17-4. *Proc. Natl. Acad. Sci. USA* **106**, 11925–30 (2009).
33. Rasband, W. S. & ImageJ, U. S. National Institutes of Health, Bethesda, Maryland, USA, [\(http://imagej.nih.gov/ij/\(1997–2014\)\)](http://imagej.nih.gov/ij/(1997–2014)) (Date of access: 10/12/09).
34. Baaske, P., Wienken, C. J., Reineck, P., Duhr, S. & Braun, D. Optical thermophoresis for quantifying the buffer dependence of aptamer binding. *Angew. Chem. Int. Ed. Engl.* **49**, 2238–2241 (2010).

Acknowledgments

The gene for DmOR85b was a gracious gift from C.W. Luejche's lab. The authors wish to thank S. Duhr and M. Jerabek-Willemsen at NanoTemper Technologies GmbH for valuable input on Microscale thermophoresis experiments and wish to thank P. Fatti, P. Gaylard, and DMSA Statistical Consultants for helpful discussion regarding the data analysis. This work was partially funded by DARPA QuBE N66001-10-1-4062, and the Yang Trust Fund. LTT gratefully acknowledges postdoctoral fellowships from the WennerGren Foundation and the Swedish Chemical Society. KC gratefully acknowledges postdoctoral fellowships from the Yang Trust Fund and the Claude Leon Foundation.

Author contributions

L.T.T., K.C. and S.Z. designed the experiments. L.T.T., K.C., J.H., B.W. and Y.Y. performed the experiments. L.T.T. and K.C. analyzed the data, wrote the manuscript, and did the figures. All authors reviewed the manuscript.

Additional information

Supplementary information accompanies this paper at <http://www.nature.com/scientificreports>

Competing financial interests: The authors declare no competing financial interests.

How to cite this article: Tegler, L.T. *et al.* Cell-free expression, purification, and ligand-binding analysis of *Drosophila melanogaster* olfactory receptors DmOR67a, DmOR85b and DmORCO. *Sci. Rep.* **5**, 7867; DOI:10.1038/srep07867 (2015).



This work is licensed under a Creative Commons Attribution-NonCommercial-ShareAlike 4.0 International License. The images or other third party material in this article are included in the article's Creative Commons license, unless indicated otherwise in the credit line; if the material is not included under the Creative Commons license, users will need to obtain permission from the license holder in order to reproduce the material. To view a copy of this license, visit <http://creativecommons.org/licenses/by-nc-sa/4.0/>